DOI: 10.1002/ejic.201100488

Solution-Stable Triple Helicates of Quaterimidazole: Three-Dimensional Crystal Structures and Optical Resolution by Chiral-Column HPLC

Yumi Yakiyama,[a] Tsuyoshi Murata,[a] Tomoaki Ise,[b] Daisuke Shiomi,[b] Kazunobu Sato,[b] Takeji Takui,*[b] Kazuhiro Nakasuji,[a] and Yasushi Morita*[a]

Keywords: Helical structures / Chiral resolution / Hydrogen bonds / Self-assembly

Complex formation of quaterimidazole with Fe^{II}, Co^{II}, and Ni^{II} yielded dinuclear triple helicates in the solution state by the self-assembling ability of the ligand based on the strong chelating coordination bonds. Crystallization of the Co^{II} complex from aqueous solution afforded the Co^{III} complex with a triple-helical structure. X-ray crystal structure analyses revealed that the helicates are linked through N–H···X hydrogen bonds with counteranions and solvent molecules to form three-dimensional networks. The spectrophotometric titration experiment showed that quaterimidazole forms triple helicates with various d-block transition metal ions with high selectivity. The outward intermolecular interactions and high stability of the helicates from the rigid molecular structures combined with the intramolecular π–π interactions of imidazole moieties and their strong chelating coordination enabled the successful optical resolution of right- and left-handed helicates by chiral-column HPLC.

Introduction

Chirality, exemplified by the double helices of DNA and α-helices of proteins, plays a pivotal role for life activity. A helicate is a supramolecular[1] helical-structured metal complex formed through the self-assembling coordination process of ligands with metal ions, and a number of helicates with d- and/or f-block transition metal ions have been investigated over the last couple of decades.[2–4] One of the most notable features of helicates is that they intrinsically possess right- (*P*) and left-handed (*M*) helical chiralities along the helical symmetry axis. Efficient use of the helical chirality can give new optical, magnetic, and electronic molecular systems.[5] The helicate formed by an achiral ligand usually affords a racemic mixture of the (*P*) and (*M*) enantiomers. In this context, optical resolution is indispensable in the quest for helicate-based chiral materials. However, only a few cases of the optical resolution of racemic mixtures of helicates have been demonstrated; spontaneous chiral crystallization[6] and chromatographic separation by using SP-Sephadex C25 with a chiral eluent.[7]

Generally, the methods above bear some intrinsic difficulties and are inappropriate because of problems in obtaining successful resolutions, time-consuming processes and/or the necessity for expensive chiral solvents or additives. Hannon and co-workers demonstrated the optical resolution of triple helicates of bis(pyridylimine) derivatives by using a cellulose column and an achiral eluent.[8] However, liquid chromatography using cellulose as the stationary phase is usually time-consuming and is therefore not a conventional method. Optical resolution using chiral-column HPLC, which does not need a long time nor expensive chiral solvents or additives, is widely believed to be the most facile and efficient approach to obtain chiral materials.[9] Any possible method for the optical resolution of helicates using the HPLC method is of great benefit to the development of helicate science. However, the optical resolution of helicates using commercially available chiral-column HPLC has never been reported except for the case of bis(dipyrrin) helicates, in which anionic ligands form very robust coordination bonds.[10] In the chromatographic method, each enantiomer can be distinguished by the difference in degree of the interaction between the chiral entity supported on a fixed-bed and the two enantiomers in solution. Obviously, functional groups on the outside of the helicate greatly affect the chiral recognition, and it is expected that the introduction of outward interaction sites into a helicate is of great benefit to the successful optical resolution using the chiral-column HPLC. At the same time, the high stability in the solution state is a key in preventing the helicate from undergoing dissociation causing chiral inversion throughout the entire process of chromatographic manipulation. It is known that both the multiple metal centers and the rigid molecular structure of ligand strengthen the structures of triple helicates, and thus their stability.[11] Such a rigidness

[a] Department of Chemistry, Graduate School of Science, Osaka University,
Toyonaka, Osaka 560-0043, Japan
Fax: +81-6-6850-5395
E-mail: morita@chem.sci.osaka-u.ac.jp
[b] Departments of Chemistry and Materials Science, Graduate School of Science, Osaka City University,
Sumiyoshi-ku, Osaka 558-8585, Japan
Fax: +81-6-6605-2522
E-mail: takui@sci.osaka-cu.ac.jp
Supporting information for this article is available on the WWW under http://dx.doi.org/10.1002/ejic.201100488.

of the polynuclear triple helicate exhibits great benefit to the kinetic inertness in the solution state, as demonstrated in the study of the bis[1-methyl-2-(5′-methylpyrid-2′-yl)-benzimidazol-5-yl]methane–Co^{II} helicate.[11]

The imidazole ring system is widely recognized as a useful building block for assembled metal complexes because of its two-directional hydrogen bonds (H-bonds) and coordination bonds. Utilizing these noncovalent interactions, we demonstrated the formation of multi-dimensional network structures on oligo(imidazole)s[12,13] and various imidazole derivatives.[14] Furthermore, our study on the crystal structures of metal complexes of 4,4′-biimidazole (**Bim**, Figure 1) showed their high ability to form H-bonded supramolecular architectures.[12b,12e] The pseudo-octahedral coordination mode in **Bim**–Ni^{II} complexes, obtained by the chelating coordination of three **Bim** moieties, reminds us of those in triple helicates of oligo(bipyridine)s.[1a] Inspired by these preceding studies, we have investigated the complex formation of 4,4′:2′,2′′:4′′,4′′′-quaterimidazole (**Qim**, Figure 1) with various transition metal ions. As a result, we have recently found that **Qim** has a high potential as a ligand for triple helicates embedding Mn^{II} or Zn^{II}.[15] The outward H-bonding sites (N–H groups) and high stability of the triple helicate in solution enabled us to prepare magnetically diluted crystals in various mixing ratios of the Mn^{II}/Zn^{II} systems, claiming the first electron-spin-based Lloyd model[16] for scalable matter spin qubits, where open-shell entities with nonequivalent *g*-tensors originating from different magnetic environments are spatially aligned.[15] In this context, (oligo)imidazole links supramolecular chemistry to quantum computing and quantum information processing. These salient molecular/electronic functionalities of **Qim**-based helicates, originating from the formation of outward N–H H-bonds, inspired us to undertake the challenge to obtain the optical resolution of the helicate by the chiral-column HPLC method. It is noteworthy that the chirality is relevant to additional qubit resources of helicates.[16,17] In this study, we show for the first time the synthesis and crystal-structure analysis of triple helicates of **Qim** with d-block transition metal ions, Fe^{II} (**1**), Co^{II} (**2**), Co^{III} (**3**), and Ni^{II} (**4**), and their optical resolution by the facile chiral-column HPLC method.

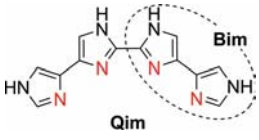

Figure 1. Molecular structure of 4,4′:2′,2′′:4′′,4′′′-quaterimidazole (**Qim**). The broken ellipse denotes the unit of 4,4′-biimidazole (**Bim**).

Results and Discussion

The complexes **1**, **2**, and **4** were obtained as racemic mixtures by mixing **Qim** with 0.67 mol-equiv. of metal sources [$Fe^{II}(ClO_4)_2{\cdot}H_2O$, $Co^{II}Br_2$ and $Ni^{II}(ClO_4)_2{\cdot}6H_2O$, respectively] in MeOH. FAB- and ESI-MS spectra in MeOH suggested the formation of the complexes with a ratio of **Qim**/metal ions = 3:2; $\{[Fe^{II}_2(\mathbf{Qim})_3]^{4+} - 3\ H^+\}$ (*m*/*z* = 907), $\{[Co^{II}_2(\mathbf{Qim})_3]^{4+} - 3\ H^+\}$ (*m*/*z* = 913) and $\{[Ni^{II}_2(\mathbf{Qim})_3]^{4+} - 3\ H^+\}$ (*m*/*z* = 911) species (Figures S1 and S2).[18] The vapor diffusion method of the MeOH solution using ethyl acetate and acetone afforded colorless single crystals of **1** and **2** suitable for X-ray analysis, respectively. When acetone/water was used as the solvent for the crystallization of **2**, the complex changed to the Co^{III} complex **3** (orange crystals) probably as a result of air oxidation. The single crystals of **4** obtained by slow concentration of its aqueous solution were reddish purple.

X-ray crystallographic analyses revealed the triple-stranded helical structures for all the $[\mathbf{M}_2(\mathbf{Qim})_3]$ complexes (Figure 2, Ni^{II} complex **4**). The complexes are racemic mixtures of the (*P*)- and (*M*)-triple helicates, which are related by inversion symmetry to each other in the unit cell. In these triple-helical structures, three **Qim** ligands show large torsion angles (68–89°, Table 1) about the central C–C bond, which connects two **Bim** units. The metal centers have pseudo-octahedral coordination geometries composed of the coordination from three **Bim** units. The coordination bond lengths and N–M–N angles in **1**, **2**, and **4** are similar to each other and also to those in $[M_2(\mathbf{Qim})_3]^{4+}$ helicates (M = Mn^{II}, Zn^{II})[15] (Table 1). The coordination environments in **4** are very similar to those of the $[Ni^{II}(\mathbf{Bim})_3]^{2+}$ complexes,[12e] acquiring the rigid coordination ability of **Qim**. The valency of the Co^{III} ion in **3** was confirmed by the short Co–N distances and large N–M–N bite angles (Table 1). The diamagnetic feature of **3** in the static magnetic measurements also shows that the Co ion in this complex has a 3+ charge with a low-spin state (Figure S3).[18] The metal–metal distances in the helicates are ca. 5 Å for all the complexes **1**–**4** (Figure 2 and Table 1). In addition, as observed in our previous study,[15] π-stacking interactions between the two imidazole rings in adjacent **Qim** ligands stabilize the triple helicate (Figure 2, shown by a two-headed thick arrow; see also Figure S4).[18] The face-to-face

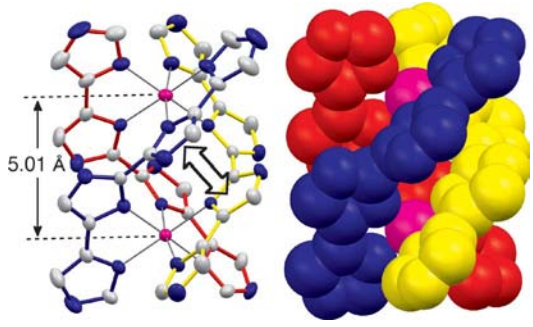

Figure 2. Triple-stranded helical structure in **4** with the anisotropic temperature factor of 50% probability (left) and space-filling model (right). Only the (*P*) enantiomer is shown. In the structure with the temperature factor, atoms are presented in specific colors as follows; C, gray; N, blue; Ni^{II}, magenta. Bond colors correspond to those of the space-filling model. The two-headed thick arrow shown between the blue and yellow imidazole rings represents the π-stacking interaction.

Table 1. Selected bond lengths [Å] and angles [°] for complexes **1**–**4**.

	M···M [Å]	M–N [Å]	N–M–N [°]	Torsion angle [°]
1	5.149(2)	2.162(7), 2.177(8), 2.166(9), 2.178(6), 2.166(6), 2.245(6), 2.172(6), 2.213(7), 2.195(6), 2.150(9), 2.215(8), 2.171(7)	76.9(3), 76.9(3), 77.5(2), 75.3(3), 77.4(3), 77.3(3)	89.3, 83.1, 69.4
2	5.135(2)	2.138(7), 2.141(8), 2.118(9), 2.166(7), 2.091(8), 2.160(7), 2.093(7), 2.108(7), 2.210(6), 2.110(8), 2.129(8), 2.114(8)	77.3(3), 78.5(3), 78.9(3), 78.3(3), 78.5(3), 78.6(3)	85.4, 67.7, 88.5
3	4.937(2)	1.922(5), 1.941(5), 1.918(6), 1.942(5), 1.905(6), 1.946(5), 1.930(5), 1.924(5), 1.941(5), 1.914(6), 1.945(5), 1.910(6)	82.9(2), 83.1(2), 83.1(3), 82.9(2), 82.9(3), 82.7(2)	72.9, 74.2, 81.7
4	5.006(1)	2.087(5), 2.094(4), 2.100(5), 2.132(4), 2.066(5), 2.125(4), 2.091(4), 2.106(4), 2.114(4), 2.091(4), 2.141(4), 2.090(4)	79.1(2), 79.5(2), 79.7(2), 78.7(2), 79.2(2), 79.2(2)	87.6, 72.6, 69.6

distances of the imidazole rings (ca. 3.4 Å) are almost the same as the sum of the C–C van der Waals radii.

All the triple helicates of **Qim** possess a salient common feature, i.e. capability of constructing a network structure by both multi-directional inter-helicate H-bonds and π-stacks. Figure 3 shows the characteristic assembled structures in complexes **1**–**4**. In the crystal structures of **1** and **4**, double N–H···O–Cl–O···H–N H-bonds with ClO_4^- and π-stacks on the **Bim** units connect the complexes to form one-dimensional structures with linear and zig-zag shapes, as shown in Figure 3a and d, respectively. The (*P*)- and (*M*)-triple helicates are aligned alternately in these one-dimensional chains. In the case of complex **2**, the double N–H···Br···H–N H-bonds connect the helicates to form a one-dimensional structure composed of one of the (*P*) or (*M*) isomer chains (Figure 3b). The three-way N–H···Br H-bonds with Br^- and the N–H···O···H–N H-bonds with MeOH connect the chains of the (*P*)- and (*M*)-helicates. In the Co^{III} complex **3**, the N–H···N H-bond directly connects the helicates, forming a one-dimensional linear chain (Figure 3c). One of the **Qim** ligands is deprotonated (Qim^-) in **3** as proved by the formation of an N–H···N H-bond with the neighboring helicates. Since the C–N–C angles of N atoms, which are sensitive to protonation, are close to each other [109(1)° and 110(1)°] in the N–H···N H-bond, the proton is disordered between the two N atoms. These H-bonded structures in **1**–**4** are further connected by multiple H-bonds across counteranions and solvent molecules, constructing three-dimensional networks. It should be noted that exchange or magnetic dipolar interactions between open-shell metal ions embedded in the helicate are expected to be quite weak because of the long intra- (ca. 5 Å) and inter-helicate M–M distances (>8 Å). These structural tendencies to form inter-helicate H-bonds (outward H-bonds) and π-stacking interactions originating from the imidazole skeletons were also observed in the Mn^{II}- and Zn^{II}-centered ones.[15] Indeed, the salient structural feature with robust triple strands afforded the first model for Lloyd's electron-spin qubits composed of Mn^{II} ions, which are weakly exchange-coupled in a one-dimensional manner and capable of *g*-tensor engineering because of the helical symmetry with the pseudo-octahedral environment around the open-shell ion.[15]

We have investigated the complexation behavior of **Qim** by means of spectrophotometric titration of **Qim** with $Co^{II}Br_2$ or $Ni^{II}(ClO_4)_2$ in MeOH solution (Figure S5).[18] In the case of the Co^{II} complex, the absorptions at 222 and 308 nm drastically decreased with increasing the Co^{II} con-

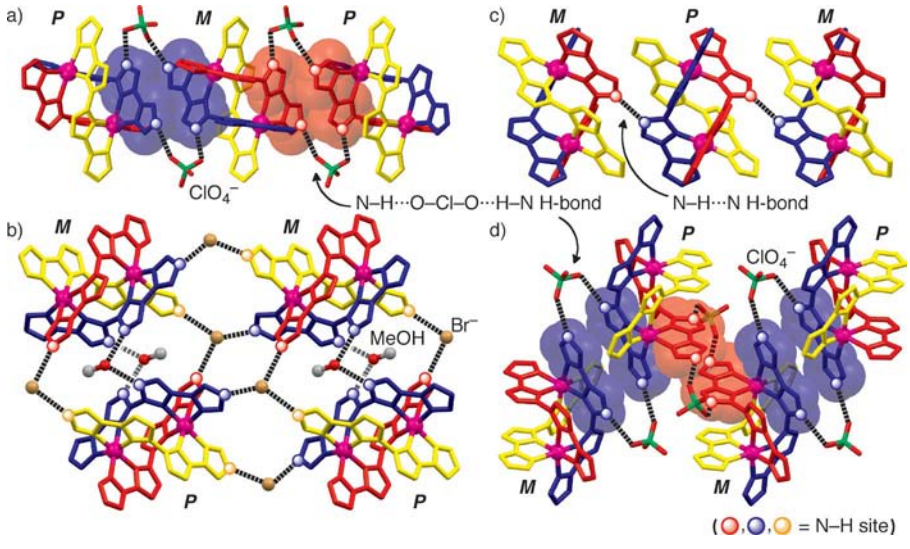

Figure 3. H-bonded structures of **Qim** helicates; (a) one-dimensional chain in **1** through ClO_4^-, (b) two-dimensional H-bonded sheet in **2**, (c) one-dimensional linear chain in **3** by direct N–H···N H-bonds, and (d) one-dimensional zig-zag structure in **4** formed by H-bonds with ClO_4^-. (*P*) and (*M*) show the right- and left-handed helicates, respectively. **Bim** units drawn in the space-filling model form the π-stacks with neighboring helicates. Dotted lines denote N–H···X H-bonds.

centration, and that at 246 nm increased accompanied by a slight redshift. The appearance of four clear isosbestic points at 207, 227, 275, and 359 nm indicates that there is mainly an excess amount of ligand and the resulting complex in the reaction mixture. Sequential changes of the absorption intensities indicate that the strong self-assembling ability of **Qim** causes the selective formation of the triple helicates. The absorptions at 225 and 307 nm exhibit minimums at an addition of ca. 0.6 equiv. of the metal source, which corresponds to a ratio of **Qim**/Co^{II} = 3:2 in the triple helicates. Further addition of Co^{II} does not cause any change in the spectra. The complex formation with Ni^{II} shows a very similar behavior in the addition range of 0.0–0.5 equiv. of Ni^{II} (Figure S5b).[18] When 0.5 equiv. of Ni^{II} is added, the absorbance at 308 nm shows a minimum. The inconsistency in the minimum point of titration (0.5 equiv.) and stoichiometry of the helicate (0.67 equiv.) is probably due to the generation of complexes with different stoichiometries such as $[Ni^{II}(\mathbf{Qim})_3]^{2+}$, a precursor of the dinuclear triple helicate. After the addition of 0.5 equiv. of Ni^{II}, a weak band at around 330 nm appears, indicating that a small amount of the complex with a different stoichiometry exists in solution.[19] The binding constants calculated from the titration spectra are in the order of 10^{19}–10^{20} M^{-4}, which are close to those of reported dinuclear triple helicates[20] and also to those of **Qim**–Mn^{II} and **Qim**–Zn^{II} complexes.[15] These results indicate that **Qim** exhibits an intrinsically high selectivity to form dinuclear triple helicates with metal ions that have an octahedral coordination sphere, although the generation of a small amount of different products was detected.

As shown by X-ray crystal structure analysis, MS, and spectrophotometric studies, the triple helicates of **Qim** have great benefits for the optical resolution by HPLC with a chiral column. We performed the optical resolution of **3** and **4**, since low-spin Co^{III} complexes exhibit considerable kinetic inertness,[21] and Ni^{II} ions are known to form the most inert complexes among the bivalent d-block transition metal ions.[22] HPLC experiments were performed by using chiral columns with various kinds of chiral stationary phases and mobile phases.[23,24] The successful resolution was only obtained for the amino acid–1-(α-naphthyl)ethylamine-supported columns. This result indicates that not only the outward H-bonds but also the π–π interactions between the ligand and the naphthyl group greatly affect the chiral separation of $[M_2(\mathbf{Qim})_3]$ helicates. The best conditions for the optical resolution of **3** and **4** were achieved when the chiral selector of (*S*)-indoline-2-carboxylic acid–(*S*)-1-(α-naphthyl)ethylamine (SUMICHIRAL OA-4800) and the mobile phase of a 70:20:10:0.05 mixed solution of hexane/EtOH/MeOH/TFA were used.[23] It should be noted that the concentration of TFA and the column temperature are also critical factors in the separation by chiral-column HPLC.[24]

The solutions of helicates in MeOH were loaded onto a chiral column and eluted with a mixed solution of hexane/EtOH/MeOH/TFA. The chromatogram showed two large and clear bands of Peak 1 and 2 (insets of Figure 4). Each fraction was directly subjected to ESI-MS, UV/Vis, and circular dichroism (CD) spectroscopy. The ESI-MS and UV/Vis spectra (Figures 4, S6 and S7)[18] show almost the same features as those of the racemic mixtures, indicating that both fractions include the $[M_2(\mathbf{Qim})_3]$ helicates, and that these triple helicates are preserved under these conditions. In the CD spectrum, the Peak 1 fraction of **3** shows positive Cotton effects at <210, 270, 318, and ca. 400 nm, and negative ones at 236 and 292 nm (Figure 5a, red line). The

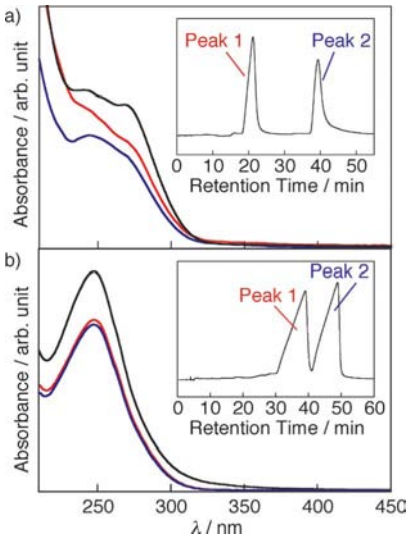

Figure 4. UV/Vis spectra of **3** (a) and **4** (b); racemic complex in MeOH (black solid line) and HPLC fractions [red line: first fraction (Peak 1); blue line: second fraction (Peak 2)]. The inset shows a chromatogram in optical resolution by using UV detection at 254 nm. Since the concentrations of the racemic helicates in MeOH and HPLC fractions are different, the absorbance in the UV/Vis spectra cannot be compared. Whereas the spectra of the HPLC fractions are measured as obtained, the similar intensities of Peaks 1 and 2 indicate that these fractions have the same amount of the helicates.

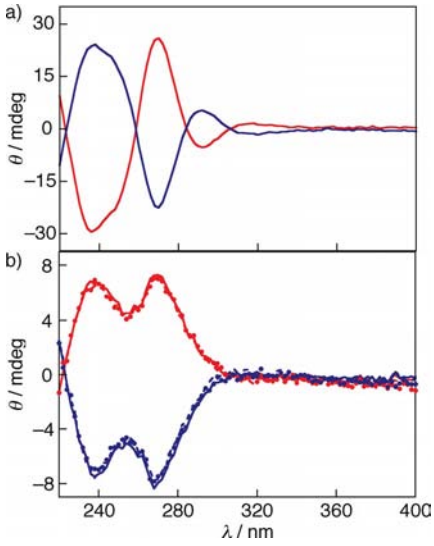

Figure 5. CD spectra of each HPLC fraction of **3** (a) and **4** (b) (0 h, solid lines; 6 h, broken lines; 1 week, dots; red and blue colors correspond to Peaks 1 and 2, respectively) in a hexane/EtOH/MeOH/TFA (70:20:10:0.05) mixed solution.

Peak 1 fraction of **4** shows two positive Cotton effects at 238 and 269 nm, and one negative Cotton effect at <210 nm (Figure 5b, red solid line). The CD spectra of Peak 2 of both **3** and **4** give exactly the mirror images of those of Peak 1 (Figure 5, blue solid lines). According to the experimental and theoretical study performed by Telfer and co-workers, these CD signals arise from intra- and internuclear exciton coupling.[7f] These results clearly illustrate that each fraction contains the (*P*) or (*M*) enantiomer of the $[M_2(\mathbf{Qim})_3]$ helicates. Notably, the intensities of the CD spectra of $[Ni^{II}_2(\mathbf{Qim})_3]^{4+}$ are preserved over a week at room temperature (Figure 5b, broken lines and dots), indicating that the chiral inversion originating from dissociation of the complex does not occur for these helicates. This result is caused by the high stability of the helicates because of the rigidness of the ligand, intra-helicate π-stacks, and strong coordination bonds characteristic of chelating coordination.[11] This observation shows that the $[M_2(\mathbf{Qim})_3]$ helicates are stable even under acidic conditions including a small amount of TFA. However, after the evaporation of the solvent, the CD intensities of the residual compounds became smaller than those of fresh samples, indicating the occurrence of racemization and/or dissociation of the triple helicates, probably because of the increased concentration of TFA by the evaporation of more volatile solvents.[25] In order to circumvent the racemization/dissociation, we have neutralized both fractions by adding an Et_3N/MeOH solution before the concentration procedure. The CD, UV, and ESI-MS spectra of the sample are almost the same as those obtained before the neutralization (Figures S8 and S9).[18] This result clearly shows that the chiral entities of $[Ni^{II}_2(\mathbf{Qim})_3]^{4+}$ are successfully isolated.[26]

Conclusions

We have revealed the intriguing features of **Qim** metal complexes: (1) the formation of the triple helicates with various d-block transition metal ions with high selectivity, (2) the self-assembling ability to construct three-dimensional networks through multiple N–H···X H-bonds and π-stacks. We emphasize that the inter-helicate H-bond formation to construct three-dimensional networks is rare among a large number of previously reported helicates.[7b,7c,27] Furthermore, we have for the first time achieved the optical resolution of the (*P*) and (*M*) enantiomers of triple helicates composed of the achiral and neutral ligand by the chiral-column HPLC method instead of simple LC. The outward N–H···X H-bonds and intermolecular π-stacks observed in the crystal structures enable the helicates to interact with chiral substrates on the column, causing the successful optical resolution of the (*P*) and (*M*) enantiomers. Also, the high stability of the helicates in solution from the rigid structure of the ligand, combined with the strong chelate coordination and intra-helicate π-stacks of the ligands prevent the helicates from chiral inversion, playing a vital role in the isolation of each enantiomer.

The chiral-column HPLC is a facile and universal method to obtain chiral materials, and the present results open a useful and powerful methodology for the optical resolution of helicates. We emphasize that the present results claim a novel concept for the development of helicate-based materials sciences. Furthermore, the expansion of the molecular diversity of the ligands gives the potentialities for the discovery of novel phenomena and functions based on chiral helicates. Further exploration of the ligands with various functions is important for the development of biological and materials sciences based on helicates. The intriguing features of oligo(imidazole)s are not only the formation of the helicates with outward intermolecular interactions but also the diversity of the network structures that are controllable by the connectivity of the imidazole rings and protonated states, as demonstrated in our previous studies.[12,13]

Because of the advantages of oligo(imidazole)-based helicates, they have marked an important milestone in studying the magneto-chiral dichromic effect and electrical magneto-chiral anisotropy.[28] It is noteworthy that the helical chirality is also important for implementing photon-linked matter qubits in quantum information processing.[15] Our ongoing studies on the (oligo)imidazole-based helicates; preparation of magnetically diluted chiral crystals for synthetic electron-spin qubits, synthesis of novel helicates composed of longer (oligo)imidazoles, f-block helicates, and hetero-multimetallic helicates, and functionalization by the introduction of redox-active substituents and electronic-spin-delocalized neutral radical systems,[29] are in progress.

Experimental Section

Materials: Qim was prepared according to our previous paper,[12a] and metal sources and solvents were used as purchased.

Preparation of $\{[Ni^{II}_2(Qim)_3](ClO_4)_4\}\cdot(H_2O)_9$ (4): $Ni^{II}(ClO_4)_2\cdot 6H_2O$ (80.3 mg, 0.21 mmol) was added to a stirred solution of **Qim** (83.7 mg, 0.31 mmol) in MeOH (15 mL). After refluxing for 30 min, the solution was cooled to room temperature and concentrated under reduced pressure. The residue was reprecipitated with MeOH/ethyl acetate to afford a soft pink powder (113.2 mg, 82% yield). The Ni^{II} complex was recrystallized from H_2O by using the slow concentration method, giving reddish-purple crystals. M.p. >300 °C (dec.). UV/Vis (MeOH): λ_{max} = 250 nm; (KBr): λ_{max} = 248 nm. $C_{36}H_{30}Cl_4N_{24}O_{16}Ni_2(H_2O)_9$ (1476.12): calcd. C 29.29, H 3.28, N 22.77; found C 29.16, H 3.03, N 22.50.

$\{[Fe^{II}_2(Qim)_3](ClO_4)_4\}\cdot(CH_3OH)_2\cdot(H_2O)$ (1): Light gray powder, 42% yield. Colorless crystals suitable for X-ray crystal structure analysis were obtained by the aerial solvent evaporation from MeOH/EtOAc solution. M.p. >300 °C (dec.). UV/Vis (MeOH): λ_{max} = 245 nm. $C_{36}H_{30}Cl_4N_{24}O_{16}Fe_2(H_2O)(CH_4O)$ (1358.34): calcd. C 32.71, H 2.67, N 24.75; found C 32.81, H 2.89, N 24.61. An elemental analysis of the crystalline sample could not be carried out because only a small amount was obtained and was used for the powder sample.

$\{[Co^{II}_2(Qim)_3](Br)_4\}\cdot(CH_3OH)\cdot(H_2O)\cdot(C_3H_6O)_6$ (2): Dull green powder, 86% yield. Colorless crystals suitable for X-ray crystal structure analysis were obtained by the vapor diffusion method from MeOH/acetone. M.p. >300 °C (dec.). UV/Vis (MeOH): λ_{max} = 246 nm. $(C_{36}H_{30}Br_4N_{24}Co_2)(H_2O)_5(CH_4O)_{1.5}$ (1374.42): calcd. C 32.77, H 3.37, N 24.46; found C 32.63, H 3.06, N 24.10. An elemen-

Table 2. Crystallographic data and structure-refinement parameters for complexes **1**–**4**.

	1	**2**	**3**	**4**
Empirical formula	$C_{38}H_{40}Cl_4Fe_2N_{24}O_{19}$[a]	$C_{55}H_{72}Br_4Co_2N_{24}O_8$[a]	$C_{36}H_{48}Br_5Co_2N_{24}O_{9.5}$[b]	$C_{36}H_{48}Cl_4N_{24}Ni_2O_{25}$
M_r [g mol^{-1}]	1390.39	1634.81	1486.32	1476.13
Crystal system	monoclinic	triclinic	monoclinic	monoclinic
Space group	$P2_1/n$	$P\bar{1}$	$P2_1/c$	$P2_1/n$
a [Å]	15.777(3)	14.2133(7)	14.816(5)	14.349(2)
b [Å]	18.027(4)	15.6384(7)	20.672(8)	13.718(2)
c [Å]	21.052(4)	16.0090(9)	17.689(6)	29.535(4)
α [°]		88.333(2)		
β [°]	109.499(4)	79.979(2)	96.20(1)	96.750(2)
γ [°]		83.795(1)		
V [Å^3]	5644(2)	3483.4(3)	5386(4)	5773(1)
Z	4	2	4	4
$D_{calcd.}$ [g cm^{-3}]	1.636	1.559	1.833	1.698
μ [mm^{-1}]	0.796	2.845	4.411	0.941
T [K]	200	150	200	200
Unique reflections	12263	15836	12129	12931
Reflections used	4351	6597	5422	11988
Parameters	768	794	690	809
$R1$, wR_2 [$I > 2\sigma(I)$]	0.0974, 0.2512	0.0894, 0.2291	0.0590, 0.1259	0.0951, 0.2335
$R1$, wR_2 (all data)	0.2031, 0.3304	0.1992, 0.2962	0.1534, 0.1465	0.1016, 0.2382
GOF on F^2	0.908	1.028	0.880	1.164
Largest diff. peak, hole [e Å^{-3}]	1.200, –0.670	0.930, –0.990	0.960, –1.040	2.110, –1.250

[a] Because of the serious disorder of solvent molecules, the accurate compositions of the crystal solvent in **1** and **2** could not be determined. [b] The Br^- ion and the water molecules (Br2/O12 and Br6/O10,O11) in complex **3** are disordered, and a site-occupancy factor of 0.5 was applied for each atom.

tal analysis of the crystalline sample could not be carried out, because only a small amount was obtained and was used for the powder sample.

{[Co^{III}_2(Qim)$_2$(Qim$^-$)]Br_5}·$(H_2O)_{9.5}$ (3): Recrystallization of the Co^{II} complex by the vapor diffusion method from H_2O/acetone yielded **3** as orange crystals. M.p. >300 °C (dec.). UV/Vis (MeOH): λ_{max} = 240, 268 nm. $C_{36}H_{29}Br_5N_{24}Co_2(H_2O)_{9.5}$ (1486.32): calcd. C 29.09, H 3.26, N 22.62; found C 29.08, H 3.16, N 22.39.

Measurements: Elemental analyses were performed at the Graduate School of Science, Osaka University. UV/Vis spectra were measured for MeOH solution with a Shimadzu UV/Vis scanning spectrophotometer UV-3100PC. High-resolution fast-atom bombardment (FAB) mass spectra were measured in MeOH solution with a JEOL JMS-SX102 spectrometer. ESI-MS data were recorded from MeOH solutions with an Applied Biosystems QSTAR® Elite spectrometer. The magnetic susceptibility measurements were performed with the microcrystal samples by using a Quantum Design SQUID magnetometer MPMS-XL with an applied field of 0.1 T over the temperature range 1.9–298 K. The melting points were measured with a hot-stage apparatus and are uncorrected. CD spectra were measured with a JASCO J820 CD spectrometer.

Crystallography: X-ray crystallographic measurements were made with a Rigaku Raxis-Rapid imaging plate or Rigaku Mercury70 diffractometer with graphite-monochromated Mo-K_α (λ = 0.71075 or 0.71070 Å, respectively). Structures were determined by direct methods using the SIR2004 program.[30] Refinements were performed by full-matrix least squares on F^2 using the SHELXL-97 program.[31] All non-hydrogen atoms except for disordered solvent and counteranion molecules were refined anisotropically, and all hydrogen atoms were included but not refined. Empirical absorption corrections were applied. Selected crystal-data collection parameters are given in Table 2. CCDC-818910 (for **1**), -818911 (for **2**), -818912 (for **3**), and CCDC-782871 (for **4**) contain the supplementary crystallographic data for this paper. These data can be obtained free of charge from The Cambridge Crystallographic Data Centre via www.ccdc.cam.ac.uk/data_request/cif.

Optical Resolution and Neutralization: The chromatographic experiment was performed with a SHISEIDO NANOSPACE SI-2 with SUMICHIRAL OA4800 (4.6 mm i.d. × 25 cm). The racemic sample was dissolved in MeOH (1 mg/100 μL), and a mixed solution (hexane/EtOH/MeOH/TFA = 70:20:10:0.05) was used as the mobile phase. The flow rate of the eluent used was 1 mL/min, and the chromatogram was traced by UV detection at 254 nm. Neutralization was obtained by adjusting each fraction after chiral separation by HPLC to pH = 7.0 with an Et_3N/MeOH solution followed by in vacuo concentration procedure. The CD, UV, and ESI mass spectra for both neutralized fractions were measured as MeOH solutions. All experiments were performed at ambient temperature.

Supporting Information (see footnote on the first page of this article): FAB and ESI mass spectra, magnetic properties, spectrophotometric titration, UV/Vis and CD spectra.

Acknowledgments

This work was partially supported by Grants-in-Aid for Scientific Research (No. 20110006 and Quantum Cybernetics), FIRST Project "Quantum Information Processing Technology" and Elements Science and Technology Project from the Ministry of Education, Culture, Sports, Science and Technology, Japan, by grants of Shorai Foundation for Science and Technology, CREST Project "Molecular Spin Quantum Computers" of Japan Science & Technology, and the Global COE program "Global Education and Research Center for Bio-Environmental Chemistry" of Osaka University. We thank Professor A. Harada and Dr. H. Yamaguchi for the CD measurements, and Professor K. Hirose for fruitful discussions on the complexation behavior by means of the spectrophotometric titration.

[1] a) J.-M. Lehn, *Supramolecular Chemistry – Concepts and Perspectives*, VCH, Weinheim, **1995**; b) J. W. Steed, J. L. Atwood, *Supramolecular Chemistry*, 2nd ed., John Wiley & Sons, Chichester, **2009**.

[2] a) J.-M. Lehn, A. Rigault, *Angew. Chem.* **1988**, *100*, 1121–1122; *Angew. Chem. Int. Ed. Engl.* **1988**, *27*, 1095–1097; b) A. F. Williams, C. Piguet, G. Bernardinelli, *Angew. Chem.* **1991**, *103*, 1530–1532; *Angew. Chem. Int. Ed. Engl.* **1991**, *30*, 1490–1492; c) I. Meistermann, V. Moreno, M. J. Prieto, E. Moldrheim, E. Sletten, S. Khalid, P. M. Rodger, J. C. Peberdy, C. J. Isaac, A. Rodger, M. J. Hannon, *Proc. Natl. Acad. Sci. USA* **2002**, *99*, 5069–5074; d) A. Oleksi, A. G. Blanco, R. Boer, I. Usón, J. Aymamí, A. Rodger, M. J. Hannon, M. Coll, *Angew. Chem.* **2006**, *118*, 1249–1253; *Angew. Chem. Int. Ed.* **2006**, *45*, 1227–1231; e) M. J. Hannon, *Chem. Soc. Rev.* **2007**, *36*, 280–295; f) V. E. Campbell, X. de Hatten, N. Delsuc, B. Kauffmann, I. Huc, J. R. Nitschke, *Nature Chem.* **2010**, *2*, 684–687; g) C. Lincheneau, R. D. Peacock, T. Gunnlaugsson, *Chem. Asian J.* **2010**, *5*, 500–504; h) E. Terazzi, L. Guénée, J. Varin, B. Bocquet, J.-F. Lemonnier, D. Emery, J. Mareda, C. Piguet, *Chem. Eur. J.* **2011**, *17*, 184–195.

[3] For comprehensive overviews of helicates with d-block transition-metal ions, see: a) E. C. Constable, *Tetrahedron* **1992**, *48*, 10013–10059; b) C. Piguet, G. Bernardinelli, G. Hopfgartner, *Chem. Rev.* **1997**, *97*, 2005–2062; c) M. Albrecht, *Chem. Rev.* **2001**, *101*, 3457–3497.

[4] For a comprehensive overview of helicates containing f-block transition-metal ions, see: C. Piguet, J.-C. G. Bünzli, in *Handbook on the Physics and Chemistry of Rare Earths*, vol. 40 (Eds.: K. A. Gschneidner Jr., J.-C. G. Bünzli, V. K. Pecharsky), North-Holland, Amsterdam, **2010**, pp. 301–553.

[5] a) *Supramolecular Chirality* (Eds.: M. Crego-Calama, D. N. Reinhoudt), Springer-Verlag, Berlin, Heidelberg, **2006**; b) H. Amouri, M. Gruselle, *Chirality in Transition Metal Chemistry: Molecules, Supramolecular Assemblies and Materials*, John Wiley & Sons, Chichester, **2008**.

[6] For spontaneous optical resolution under crystallization for helicates with d-block transition-metal ions, see: a) R. Krämer, J.-M. Lehn, A. De Cian, J. Fischer, *Angew. Chem.* **1993**, *105*, 764–767; *Angew. Chem. Int. Ed. Engl.* **1993**, *32*, 703–706; b) Q. Sun, Y. Bai, G. He, C. Duan, Z. Lin, Q. Meng, *Chem. Commun.* **2006**, 2777–2779; c) A. Dobrov, V. B. Arion, S. Shova, A. Roller, E. Rentschler, B. K. Keppler, *Eur. J. Inorg. Chem.* **2008**, 4140–4145; for spontaneous optical resolution under crystallization for helicates with f-block transition-metal ions, see: d) P. Gawryszewska, J. Legendziewicz, Z. Ciunik, N. Esfandiari, G. Muller, C. Piguet, M. Cantuel, J. P. Riehl, *Chirality* **2006**, *18*, 406–412; optical resolution by the formation of a diastereomer ion pair was reported on boron–sodium helicates, although the helicates do not contain transition-metal ions, see: e) H. Katagiri, T. Miyagawa, Y. Furusho, E. Yashima, *Angew. Chem.* **2006**, *118*, 1773–1776; *Angew. Chem. Int. Ed.* **2006**, *45*, 1741–1744; f) K. Miwa, Y. Furusho, E. Yashima, *Nature Chem.* **2010**, *2*, 444–449.

[7] For chromatographic optical resolution with SP-Sephadex C25 for helicates with d-block transition-metal ions, see: a) L. J. Charbonniere, G. Bernardinelli, C. Piguet, A. M. Sargeson, A. F. Williams, *J. Chem. Soc., Chem. Commun.* **1994**, 1419–1420; b) B. Hasenknopf, J.-M. Lehn, *Helv. Chim. Acta* **1996**, *79*, 1643–1650; c) G. Rapenne, B. T. Patterson, J.-P. Sauvage, F. R. Keene, *Chem. Commun.* **1999**, 1853–1854; d) C. R. K. Glasson, G. V. George, J. K. Clegg, L. F. Lindoy, J. A. Smith, F. R. Keene, C. Motti, *Chem. Eur. J.* **2008**, *14*, 10535–10538; dinuclear f–d block helicates were prepared by addition of lanthanide ions after SP-Sephadex C25 chromatography of the mononuclear Cr^{III} complex, see: e) M. Cantuel, G. Bernardinelli, G. Muller, J. P. Riehl, C. Piguet, *Inorg. Chem.* **2004**, *43*, 1840–1849; f) S. G. Telfer, N. Tajima, R. Kuroda, M. Cantuel, C. Piguet, *Inorg. Chem.* **2004**, *43*, 5302–5310.

[8] For chromatographic optical resolution with a cellulose column for helicates with d-block transition-metal ions of bis(pyridylimine) ligands, see: a) M. J. Hannon, I. Meistermann, C. J. Isaac, C. Blomme, J. R. Aldrich-Wright, A. Rodger, *Chem. Commun.* **2001**, 1078–1079; b) J. M. C. A. Kerckhoffs, J. C. Peberdy, I. Meistermann, L. J. Childs, C. J. Isaac, C. R. Pearmund, V. Reudegger, S. Khalid, N. W. Alcock, M. J. Hannon, A. Rodger, *Dalton Trans.* **2007**, 734–742; c) H. Yu, X. Wang, M. Fu, J. Ren, X. Qu, *Nucleic Acids Res.* **2008**, *36*, 5695–5703.

[9] a) L. Miller, C. Orihuela, R. Fronek, D. Honda, O. Dapremont, *J. Chromatogr. A* **1999**, *849*, 309–317; b) N. M. Maier, P. Franco, W. Lindner, *J. Chromatogr. A* **2001**, *906*, 3–33.

[10] Enantiomers of single- or double-helicates of bis(dipyrrin) derivatives composed of achiral and anionic ligands forming very robust coordination bonds were separated by chiral-column HPLC with silica-based chiral stationary phases immobilizing with D-phenylglycine, cellulose or amylose derivatives, see: a) M. Bröring, C. D. Brandt, J. Lex, H.-U. Humpf, J. Bley-Escrich, J.-P. Gisselbrecht, *Eur. J. Inorg. Chem.* **2001**, 2549–2556; b) T. E. Wood, N. D. Dalgleish, E. D. Power, A. Thompson, X. Chen, Y. Okamoto, *J. Am. Chem. Soc.* **2005**, *127*, 5740–5741; see also the helicates with chiral ligands: c) T. E. Wood, A. C. Ross, N. D. Dalgleish, E. D. Power, A. Thompson, X. Chen, Y. Okamoto, *J. Org. Chem.* **2005**, *70*, 9967–9974; d) A. A.-S. Ali, R. E. Benson, S. Blumentritt, T. S. Cameron, A. Linden, D. Wolstenholme, A. Thompson, *J. Org. Chem.* **2007**, *72*, 4947–4952.

[11] a) L. J. Charbonnière, M.-F. Gilet, K. Bernauer, A. F. Williams, *Chem. Commun.* **1996**, 39–40; b) L. J. Charbonnière, A. F. Williams, U. Frey, A. E. Merbach, P. Kamalaprija, O. Schaad, *J. Am. Chem. Soc.* **1997**, *119*, 2488–2496.

[12] a) Y. Morita, T. Murata, S. Yamada, M. Tadokoro, A. Ichimura, K. Nakasuji, *J. Chem. Soc. Perkin Trans. 1* **2002**, 2598–2600; b) Y. Morita, T. Murata, K. Fukui, M. Tadokoro, K. Sato, D. Shiomi, T. Takui, K. Nakasuji, *Chem. Lett.* **2004**, *33*, 188–189; c) Y. Morita, T. Murata, K. Fukui, S. Yamada, K. Sato, D. Shiomi, T. Takui, H. Kitagawa, H. Yamochi, G. Saito, K. Nakasuji, *J. Org. Chem.* **2005**, *70*, 2739–2744; d) T. Murata, Y. Morita, Y. Yakiyama, Y. Yamamoto, S. Yamada, Y. Nishimura, K. Nakasuji, *Cryst. Growth Des.* **2008**, *8*, 3058–3065; e) T. Murata, Y. Yakiyama, K. Nakasuji, Y. Morita, *Cryst. Growth Des.* **2010**, *10*, 4898–4905.

[13] T. Murata, Y. Morita, K. Fukui, Y. Yakiyama, K. Sato, D. Shiomi, T. Takui, K. Nakasuji, *Cryst. Growth Des.* **2006**, *6*, 1043–1047.

[14] a) T. Murata, Y. Morita, K. Fukui, K. Sato, D. Shiomi, T. Takui, M. Maesato, H. Yamochi, G. Saito, K. Nakasuji, *Angew. Chem.* **2004**, *116*, 6503–6506; *Angew. Chem. Int. Ed.* **2004**, *43*, 6343–6346; b) T. Murata, Y. Morita, Y. Yakiyama, K. Fukui, H. Yamochi, G. Saito, K. Nakasuji, *J. Am. Chem. Soc.* **2007**, *129*, 10837–10846.

[15] Y. Morita, Y. Yakiyama, S. Nakazawa, T. Murata, T. Ise, D. Hashizume, D. Shiomi, K. Sato, M. Kitagawa, K. Nakasuji, T. Takui, *J. Am. Chem. Soc.* **2010**, *132*, 6944–6946.

[16] a) S. Lloyd, *Sci. Am.* **1995**, *273*, 140–145. The differences in the magnetic environment of a trinuclear triple helicate including lanthanide ions was demonstrated in the solution state with the help of paramagnetic NMR spectroscopic measurements, see: b) N. Ouali, J.-P. Rivera, P.-Y. Morgantini, J. Weber, C. Piguet, *Dalton Trans.* **2003**, 1251–1263.

[17] K. Sato, S. Nakazawa, R. Rahimi, T. Ise, S. Nishida, T. Yoshino, N. Mori, K. Toyota, D. Shiomi, Y. Yakiyama, Y. Morita, M. Kitagawa, K. Nakasuji, M. Nakahara, H. Hara, P. Carl, P. Höfer, T. Takui, *J. Mater. Chem.* **2009**, *19*, 3739–3754.

[18] FAB and ESI mass spectra, magnetic properties, spectrophotometric titrations, UV/Vis and CD spectra are available; see Supporting Information.

[19] We investigated the complex formation by mixing **Qim** and $Ni^{II}(ClO_4)_2$ in a 1:1 ratio. In the X-ray crystal structure analysis, the resulting complex showed a triple-helical structure of

$[Ni^{II}_2(\mathbf{Qim})_3]^{4+}$ identical to that of **4**. This result indicates that the major product of the complexation is the $[Ni^{II}_2(\mathbf{Qim})_3]^{4+}$ helicate, even in the solution of a 1:1 mixture of **Qim** and Ni^{II}.

[20] a) C. Piguet, G. Bernardinelli, B. Bocquet, A. Quattropani, A. F. Williams, *J. Am. Chem. Soc.* **1992**, *114*, 7440–7451; b) L. J. Charbonnière, A. F. Williams, C. Piguet, G. Bernardinelli, E. Rivara-Minten, *Chem. Eur. J.* **1998**, *4*, 485–493.

[21] R. G. Wilkins, *Kinetics and Mechanisms of Reaction of Transition Metal Complexes*, 2nd ed., VCH, Weinheim, **1991**.

[22] F. Basolo, R. G. Pearson, *Mechanisms of Inorganic Reactions*, John Wiley & Sons, New York, **1958**.

[23] The optical resolution of $[Co^{III}_2(\mathbf{Qim})_3]^{6+}$ was examined by using silica-based chiral columns with chiral stationary phases of polysaccharide types (CHIRALPACK AD-RH, IC and CHIRALCEL OD-RH, OJ-RH), a polymethacrylate type (CHIRALPAK OP), amino acid types (SUMICHIRAL OA-2000S, 2500, 3100, 3200 and 3300), and amino acid–1-(*α*-naphthyl)ethylamine-combined types (SUMICHIRAL OA-4000, 4100, 4400, 4500, 4600, 4700, 4800 and 4900) at room temperature. Separation of the (*P*) and (*M*) enantiomers were observed only for the columns with the amino acid–1-(*α*-naphthyl)ethylamine-combined chiral stationary phases (SUMICHIRAL OA-4100, 4400, 4700, 4800 and 4900). Lowering of the column temperature resulted in a better resolution. Addition of 0.001–0.050% of TFA to the mobile phase remarkably improved the separation of the enantiomers, probably because of inhibition of the deprotonation process of the N–H groups in the **Qim** ligand.

[24] We also examined the optical resolution of the Mn^{II}, Fe^{II}, and Zn^{II} complexes. The (*P*) and (*M*) enantiomers of the Fe^{II} complex were completely separated by a SUMICHIRAL OA-4800 column and a mobile phase of hexane/EtOH/MeOH/TFA = 70:20:10:0.001. The separation of the Zn^{II} complex was partially observed at a column temperature of 10 °C by using the same chiral column and eluent for the separation of the Fe^{II} complex. The Mn^{II} complex, which is expected to be the most labile among the reported $[M^{II}_2(\mathbf{Qim})_3]^{4+}$ complexes, showed only one peak of the racemic mixture, even at 10 °C. The difficulties involved in obtaining optical resolution of the Mn^{II} and Zn^{II} complexes are probably due to the dissociation of the helicates causing the racemization.

[25] The CD intensities of the separated HPLC fractions of $[Co^{III}_2(\mathbf{Qim})_3]^{6+}$, after concentration without neutralization, reproduced those of fresh chiral samples, although some decomposition of the helicates was observed. This result indicates that the Co^{III} complex possesses a higher stability than that of the Ni^{II} complex where the HPLC fractions could not preserve their chiralities during the concentration procedure under acidic conditions.

[26] Further studies involving the identification of the absolute configuration and structural elucidation of each enantiomer are under way.

[27] For examples of helicates forming multi-dimensional networks by inter-helicate H-bonds, see: a) L. K. Thompson, C. J. Matthews, L. Zhao, C. Wilson, M. A. Leech, J. A. K. Howard, *J. Chem. Soc., Dalton Trans.* **2001**, 2258–2262; b) C. J. Matthews, S. T. Onions, G. Morata, L. J. Davis, S. L. Heath, D. J. Price, *Angew. Chem.* **2003**, *115*, 3274–3277; *Angew. Chem. Int. Ed.* **2003**, *42*, 3166–3169; c) A. Lavalette, F. Tuna, G. Clarkson, N. W. Alcock, M. J. Hannon, *Chem. Commun.* **2003**, 2666–2667; d) F. Tuna, M. R. Lees, G. J. Clarkson, M. J. Hannon, *Chem. Eur. J.* **2004**, *10*, 5737–5750; e) K. Fujita, R. Kawamoto, R. Tsubouchi, Y. Sunatsuki, M. Kojima, S. Iijima, N. Matsumoto, *Chem. Lett.* **2007**, *36*, 1284–1285; f) J. Tang, J. S. Costa, G. Aromí, I. Mutikainen, U. Turpeinen, P. Gamez, J. Reedijk, *Eur. J. Inorg. Chem.* **2007**, 4119–4122.

[28] a) G. L. J. A. Rikken, E. Raupach, *Nature* **1997**, *390*, 493–494; b) G. L. J. A. Rikken, J. Fölling, P. Wyder, *Phys. Rev. Lett.* **2001**, *87*, 236602/1–4.

[29] For our recent studies on air-stable neutral radicals with condensed cyclic structures, see: a) A. Ueda, S. Nishida, K. Fukui, T. Ise, D. Shiomi, K. Sato, T. Takui, K. Nakasuji, Y. Morita, *Angew. Chem.* **2010**, *122*, 1722–1726; *Angew. Chem. Int. Ed.* **2010**, *49*, 1678–1682; b) Y. Morita, S. Suzuki, K. Fukui, S. Nakazawa, H. Kitagawa, H. Kishida, H. Okamoto, A. Naito, A. Sekine, Y. Ohashi, M. Shiro, K. Sasaki, D. Shiomi, K. Sato, T. Takui, K. Nakasuji, *Nat. Mater.* **2008**, *7*, 48–51; c) Y. Morita, S. Nishida, J. Kawai, T. Takui, K. Nakasuji, *Pure Appl. Chem.* **2008**, *80*, 507–517; d) Y. Morita, S. Nishida, in *Stable Radicals: Fundamental and Applied Aspects of Odd-Electron Compounds* (Ed.: R. Hicks), John Wiley & Sons Ltd., Chichester, **2010**, chapter 3, pp. 81–145; e) Y. Morita, S. Suzuki, K. Sato, T. Takui, *Nature Chem.* **2011**, *3*, 197–204; f) S. Nishida, K. Kariyazono, A. Yamanaka, K. Fukui, K. Sato, T. Takui, K. Nakasuji, Y. Morita, *Chem. Asian J.* **2011**, *6*, 1188–1196.

[30] M. C. Burla, R. Caliandro, M. Camalli, B. Carrozzini, G. L. Cascarano, L. De Caro, C. Giacovazzo, G. Polidori, R. Spagna, *J. Appl. Crystallogr.* **2005**, *38*, 381–388.

[31] G. M. Sheldrick, *Acta Crystallogr., Sect. A* **2008**, *64*, 112–122.

Received: May 12, 2011
Published Online: July 8, 2011

